^{1}H MAS NMR Investigations of Ethylene Glycol Adsorbed in NaX

Özlen F. Erdem and Dieter Michel*

Institute of Experimental Physics II, University of Leipzig, D-04103 Leipzig, Germany

Received: January 25, 2005; In Final Form: April 29, 2005

The application of ^{1}H MAS NMR allows a detailed study of the behavior of ethylene glycol adsorbed in NaX zeolites which may be used to understand the effect of confinement. Typical changes in the chemical shift values for the CH_2 and OH groups were found which are very sensitive to interactions between the molecules and the internal surfaces. This allows clear differentiation between molecules within the zeolite cages and those adsorbed at the outer surface of the zeolite grains and also allows study of the dynamics of the different species. Selective ^{1}H T_1 measurements were carried out for various pore-filling degrees where large differences were found in the thermal mobility. It is shown that for the molecules inside the supercages, a dynamic heterogeneity occurs which may be related to the competing influences of molecule−internal surface interactions and molecule−molecule interactions within a network of intermolecular hydrogen bonds.

Introduction

The structure and mobility of molecules adsorbed in restricted geometry such as zeolites have been widely investigated by means of NMR spectroscopy.[1−3] Very often nuclear spins were used (e.g. ^{13}C and ^{15}N), where a sufficient spectral resolution can be achieved because of large chemical shifts and *J* coupling constants.[1] For these systems, as studied in this work, the proton chemical shifts of the adsorbed molecules are commonly much more sensitive to changes in electronic structure and surroundings than those nuclei forming the skeleton of the molecule. In the case of proton NMR spectroscopy, however, the applicability of NMR spectroscopy to molecules adsorbed on surfaces is often limited due to poor resolution. Line broadening is not only caused by restricted molecular mobility and dipole interaction of the proton spins with paramagnetic centers, but originates also from the presence of random local magnetic fields within the polycrystalline materials. A notable enhancement in resolution of the spectra may be achieved when the local magnetic fields are averaged out by the application of MAS techniques. Already moderate spinning frequencies of 3 to 6 kHz are sufficient to realize a line narrowing. In addition, translational motion of the molecules may also modulate the local magnetic fields, if the mean diffusion length $(6Dt)^{1/2}$ during the NMR measuring time $t \approx T_2$ is comparable to the mean diameter of the polycrystallite grains. Therefore, in the case of proton high-resolution (HR) NMR spectroscopy of adsorbed molecules, MAS and thermal motional effects may compete but they can be considered to be statistically independent of each other. A rigorous treatment of these influences on the NMR line shape was performed in previous work that is based on a statistical line shape theory and which takes into account a product *ansatz* for the time correlation function including MAS and thermal motion. This approach may explain the sideband pattern and the fact, for instance, that already at intermediate frequencies (near 1 kHz) well-resolved spectra with Lorentzian line shapes appear. They are characterized by a residual line width being proportional to the product of the correlation time for the thermal motion and the second moment of the static distribution of the random local fields which show quadratic dependence on the flux density B of the external magnetic field.

Because of these facts, the line shapes in the ^{1}H MAS NMR measurements as presented here are influenced by different local fields, and we may not derive unambiguous, quantitative conlusions about the dynamics of the adsorbed molecules in zeolites. Therefore, only the analysis of chemical shift appears to be useful in our study. Moreover, to characterize the dynamical behavior of the molecules and, thus, to study the guest−host interactions, the investigation of NMR relaxation is of special interest, too.[4−9] The study of the reorientational dynamics and the diffusion of adsorbed molecules[4,5] under the influence of the confinement is also important to understand changes in the collective properties, such as melting and freezing of the adsorbed molecules.[6,7] Dosseh et al.[8] investigated cyclohexane and benzene confined in the mesoporous materials MCM-41 and SBA-15 by using differential scanning calorimetry (DSC) and NMR line-shape analysis. They have reported that in pores corresponding roughly to 10 to 30 molecular sizes, important depressions of the melting point can be observed and the confined substances crystallize only partially. By means of broadband dielectric spectroscopy, Kremer et al.[10−14] investigated ethylene glycol ($HOCH_2CH_2OH$, abbreviated as EG) confined in silica-sodalite, silicalite, zeolite beta, and aluminophosphate $AlPO_4$-5. Silica-sodalite samples (cages with an inner diameter of 0.6 nm[15]) are prepared in such a way that each cage is loaded with one EG molecule. A complete loading with EG molecules was realized for silicalite/H-ZSM-5 zeolites (with a larger channel of 0.56 nm × 0.53 nm and smaller channel of 0.55 nm × 0.51 nm). Respective dielectric relaxation measurements showed an Arrhenius type temperature dependence. This dependence was attributed by Kremer et al. to a single-molecule behavior. Completely loaded sample with EG in sol−gel-glasses (pore diameter of 2.5 nm), zeolite beta (larger channel 0.56 nm × 0.53 nm and smaller pores of 0.55 nm), and $AlPO_4$-5 showed a Vogel−Fulcher−Tammann (VFT)[16,17] type temperature dependence of the (mean) dielectric relaxation rate similar to that found for the dynamics of EG in case of a bulk sample. Kremer et al. have related this change in the behavior to the coordination

* Corresponding author. E-mail: michel@physik.uni-leipzig.de. Tel.: +493419732600, Fax: +493419732649.

10.1021/jp050434m CCC: $30.25
Published on Web 05/27/2005

number for the adsorbed EG molecules: while EG in silicalite has a coordination number of four, EG in zeolite beta or $AlPO_4$-5 has a coordination number of five. The authors claimed that an ensemble as small as six molecules is sufficient for revealing a liquid-like dynamics and have estimated a characteristic length $\xi \approx 0.7$ nm. A problem in these samples is that they possess a quasi one-dimensional, interconnected system of channels and thus the topology of the system can only be described by the mean number of EG molecules per channel crossing, i.e., the internal free volume is not well-defined. This is one reason why we have used in this study NaX zeolites with well-defined dimensions of the supercages (see below).

In the work of Kremer et al.[10] a sample preparation was applied which involves injection of excess amount of EG at 10 K to 20 K less than the boiling temperature of bulk EG under vacuum, after dehydration of the zeolites and the $AlPO_4$-5. The sample was kept for at least 1 day to ensure a statistic distribution of the adsorbed molecules.[18] In this procedure, the presence of adsorbed molecules on the outer surface of the zeolites in addition to their presence in the internal cages cannot be excluded. This situation is hereafter referred to as "overloading". They have tried to get rid of these excess molecules by heating the sample up to 573 K before the measurements. Nonetheless, the quality of sample preparation has not been characterized in detail. Medick et al.[19] compared the dynamical heterogeneity in glass formers (such as EG) embedded in zeolite beta and in binary glass formers. They have performed 1D and 2D ^{2}H NMR experiments to study reorientational correlation times. By analyzing 2D NMR spectra, they were able to monitor reorientation and exchange processes separately from each other. In the case of EG adsorbed in zeolite beta, no exchange of the molecules between the cages was observed, and it was concluded that the translation of the molecules is slow with respect to the time scale of 100 ms. By using ^{1}H NMR spectroscopy, Hong et al.[20,21] investigated host−guest interactions between pure-silica and aluminosilicate sodalites as adsorbents and EG as guest molecules. Hong et al. synthesized pure-silica and aluminosilicate sodalites with EG. Differences in the chemical shifts were found when sodalites have different Si/Al ratios. The chemical shifts were interpreted in terms of the conformation of EG molecules in the beta-cages of the sodalite samples which is influenced by the formation of hydrogen bonds to the framework.

In this paper, we investigate EG molecules adsorbed in NaX zeolite by means of MAS ^{1}H NMR spectroscopy. The faujasite type zeolite NaX has a supercage diameter of 12.7 Å. These supercages are interconnected to a three-dimensional system of channels by open-twelve membered ring windows 7.4 Å in diameter.[15] This allows a free entrance of ethylene glycol molecules (with a hard core diameter of ca. 3.6 Å). The cubic unit cell contains 8 supercages. The inner pore volume of NaX was determined by nitrogen adsorption method. From molar mass calculations, a complete pore filling of NaX with EG is estimated corresponding to 10 molecules per supercage at room temperature. This is referred to as $\Theta = 1.0$. In our sample preparation route this corresponds to 30 μL of EG for 80 mg of NaX.

Obviously, a definite preparation of the samples plays a decisive role in these studies. Therefore, the first goal in our study is to realize and to characterize a reproducible preparation of the samples, where the EG molecules are confined in the restricted geometry of NaX zeolites. This can be controlled by means of the line shape in the ^{1}H NMR spectra. In this context we will show that the analysis of ^{1}H NMR spectra over a broad range of pore-filling factors allows us to differentiate between molecules in the internal cages and the ones adsorbed on the external surfaces. Hence, from the chemical shift analysis, one may study the physical and chemical properties of molecules in confined geometry. Furthermore, we present studies on the internal dynamics of the "physically trapped" molecules by means of selective ^{1}H NMR longitudinal relaxation time measurements.

Experimental Section

Methods. Variable temperature ^{1}H MAS NMR experiments were performed using a conventional MAS probe with outer rotor diameters of 7 mm and 4 mm. The measurements were run with a proton 90° pulse length of 3.3 μs and 4.8 μs at Larmor frequencies of 500 and 100 MHz, respectively. For ^{1}H NMR measurements a single 90° pulse sequence with four pulse-CYCLOPS phase cycling and for T_1 measurements the routine inversion recovery sequence were used. MAS rotation at 2 kHz was applied to reduce the (inhomogeneous) line broadening. In these measurements, we have to take into account that the temperature of the sample in the rotor depends on the rotation frequency, the diameter and the geometry of the rotor, the position of the sample volume, and the bearing gas pressure p.[22] In our experiments, we may estimate a temperature change $\Delta T/\Delta p$ of 0.13 K bar^{-1}. Hence, for measurements with a 7 mm MAS rotor, an MAS frequency of 2 kHz, and a bearing pressure of 2 bar, we estimate a value of $\Delta T \approx 0.3$ K. Hence, the expected temperature deviations are within the limits of experimental accuracy.

Sample Preparation. Approximately 0.8 and 0.3 g of NaX (Si/Al: 1.2) was filled in 7 mm and 4 mm MAS glass tubes, respectively. The samples were heated at 673 K for 48 h under vacuum with a final pressure below 10^{-5} mbar in order to remove the water and possible paramagnetic impurities. After cooling the sample to room temperature, a certain amount of EG was added to the tubes at room temperature by the aid of a syringe. The glass container consists of two interconnected parts, the smaller one for MAS studies and the larger cylindrical one for the connection with the vacuum line. Between the two parts the diameter of the interconnecting glass tube is reduced (like a capillary) to simplify the process of sample sealing. A further reduced diameter, for sealing-off, was made on the larger tube. Since the conditions during injection were not completely airtight and they did not prevent O_2 entering into the sample, immediately after injection the samples were once again attached to the vacuum line using a hose pipe. To ensure a quantitative transfer of the adsorbent, EG, into the sample, we have cooled the sample to liquid nitrogen temperature and then disconnected it from the vacuum line by sealing-off at the larger tube. After that, the total sample was kept in an oven at 373 K for 24 h to achieve a good distribution of the molecules. Finally, the sample was cooled again in liquid nitrogen and sealed-off at the small tube in a way to guarantee a fast rotation of the small capsules in the MAS NMR measurements. Moreover, IR measurements under conditions of diffuse reflection were done in order to check the influence of residual water. No evidence for residual water was found. The purity of EG was also checked by means of liquid-state HR ^{1}H NMR spectroscopy and gas chromatography coupled with mass spectroscopy.

Results

^{1}H NMR Chemical Shifts Analysis. A typical ^{1}H NMR spectrum of EG adsorbed in NaX zeolites is shown in Figure 1, which reveals a fairly good resolution achievable by the

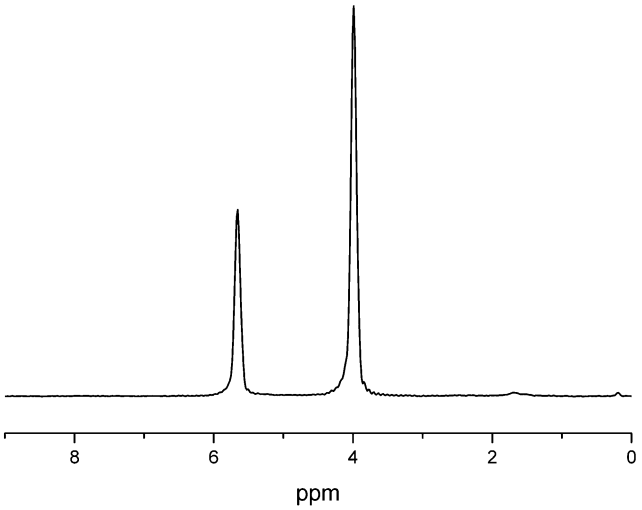

Figure 1. ^{1}H MAS NMR spectrum (500 MHz, MAS frequency of 3 kHz) of ethylene glycol (EG) in NaX taken at 295 K. An amount of ca. 34 μL of EG was adsorbed in 80 mg of NaX corresponding to ca. 11 molecules/cage (a complete filling occurs at 10 molecules/cage). The two peaks at 4.2 and 5.7 ppm (relative to liquid TMS) belong to the CH_2 and OH groups of EG, respectively.

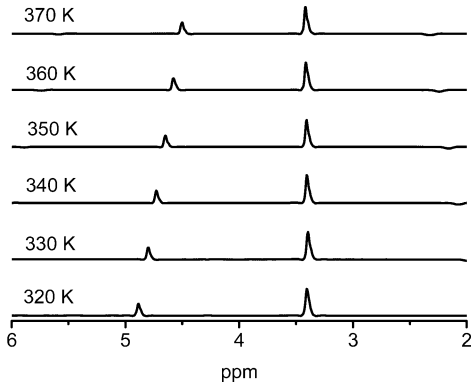

Figure 2. Temperature dependence of ^{1}H MAS NMR spectra (500 MHz, MAS frequency of 2 kHz) for bulk EG.

application of the MAS method. The two lines at 5.7 and 4.2 ppm may be simply ascribed to the OH and CH_2 groups of EG molecule, respectively. In this sample, the amount of EG adsorbed corresponds statistically to a pore-filling factor of $\Theta = 1.1$. The assumption of a statistical distribution of the molecules adsorbed in NaX seems to be justified since we have applied a longer equilibrium time after the sample preparation.

To arrive at a complete assignment of the chemical shift values, in Figure 2 the temperature dependence of the ^{1}H MAS NMR spectra (500 MHz, MAS frequency of 2 kHz) is shown for a bulk EG sample. It is well-known[23] that EG can be used for temperature calibration in NMR spectrometers. By increasing the temperature, the chemical shift of the CH_2 line remains almost constant, whereas the OH line shifts in the direction of higher fields, reducing the shift difference with the CH_2 line. This fact can be well understood because it is known that the more the intermolecular hydrogen bonds break down, the more the line shifts to higher fields.[24]

It is interesting to consider an EG/NaX sample with approximately complete pore filling, $\Theta \approx 1.0$ (Figure 3). Already at lower temperatures, two relatively narrow lines at 4.1 and 5.7 ppm are observed with an intensity ratio of ca. 1:2. The chemical shift of the more intense line at 4.1 ppm is temperature independent, and by increasing the temperature, the less intense line shifts toward higher fields in the range between 5.7 and

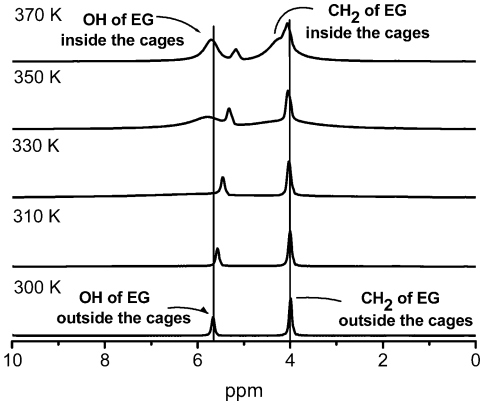

Figure 3. Temperature dependence of ^{1}H MAS NMR (500 MHz, MAS frequency of 2 kHz) for EG in NaX with $\Theta = 1.0$.

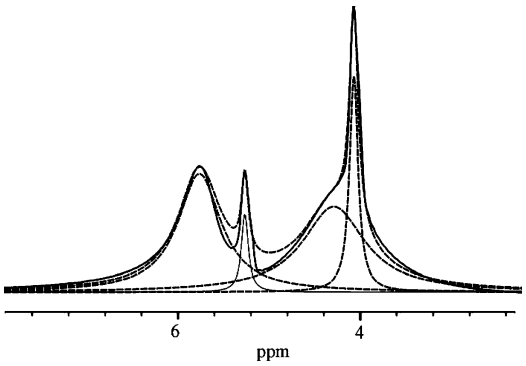

Figure 4. Deconvolution of the spectrum for $\Theta = 1.0$ taken at 360 K. The solid line stands for the ^{1}H MAS NMR spectrum, and the dashed lines are for the deconvoluted spectra. EG molecules adsorbed within the zeolite cages appear at different chemical shifts and intensities than those ones at the outer surfaces. The respective chemical shifts for the OH groups are 5.7 and 5.2 ppm and for the CH_2 groups 4.3 and 4.1 ppm.

5.2 ppm. This behavior is quite similar to that observed for EG molecules in the bulk liquid (Figure 2). This similarity allows us to attribute these two lines to OH and CH_2 groups of EG molecules which are not adsorbed in the zeolitic cages but sitting on the outer surfaces of the zeolite grains. If the temperature is increased to 360 K, besides these two sharp peaks, additional broader lines appear with chemical shifts of 5.8 and 4.4 ppm. Typical resonance shifts of these lines were observed for adsorbed EG molecules at low pore-filling factors that highly support our assignment. They show even broader lines as measured for EG molecules in samples with lower pore-filling factors. The latter fact, clearly shown in Figure 3 and for the decomposed spectrum in Figure 4, can be simply explained. In the case of "overloaded" zeolites, the molecules confined in the cages are more strongly restricted, because, for instance, the exchange between molecules outside and inside the cages is more strongly hindered. The interpretation of the different proton NMR lines is also in agreement when the pore-filling factor is appreciably less than $\Theta = 1.0$ (Figure 5). Here the narrow lines with the typical shifts for EG molecules at the outer surfaces cannot be detected.

As we are interested in a well-defined system where only molecules in the inner cages of the NaX zeolites are present, the dependence of the NMR spectra on the pore-filling factor has been studied in detail. A deconvoluted ^{1}H NMR spectrum of EG in NaX with a loading degree of $\Theta = 0.2$ is shown in Figure 5 including the relative fractions. Here, contrary to Figure 1, additional lines appear at 10, 2.5, and 1.3 ppm at 310 K. To

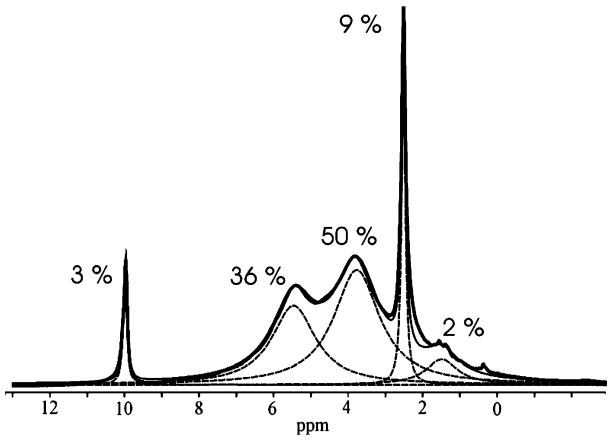

Figure 5. Deconvolution of the ^{1}H MAS NMR spectrum for $\Theta = 0.2$ (solid line) measured under the same conditions as in Figure 3.

assign the additional lines, we have prepared samples with even less loading degrees, because we may expect that under these conditions, a predominant interaction between adsorbed molecules and adsorption sites inside the supercage may take place. To prove this assumption, we have measured an NaX sample without any loading. The ^{1}H MAS NMR spectra of such a sample (not shown here) gave also a line at 1.3 ppm which is known to be typical for SiOH groups in NaX zeolites. Furthermore, a line at 5.2 ppm has been detected which is ascribed to bridged OH groups. We may assume that these SiOH groups interact with adsorbed EG molecules that lead to the appearance of a line at 2.5 ppm. The shift of the ^{1}H NMR lines for OH groups due to interaction with adsorbed molecules is well established in previous works.[24,25]

For the interpretation of the line observed at 10 ppm, one has to consider two important points: First, this line is relatively sharp in comparison with the main lines at 5.7 and 4.2 ppm. Second, ^{1}H NOESY experiments do not show any evidence of a cross-peak between the 10 ppm line and other ones, i.e., no coupling with neighboring protons. These two facts suggest that the line at 10 ppm does not belong to the species inside the supercages. According to Emmler et al.,[26] it is possible to correlate the hydrogen bond geometry, e.g. the displacement of the hydrogen bond from the exact middle of the OH···O hydrogen bond, with the experimentally measured chemical shifts. If we consider the ^{1}H MAS NMR spectrum for EG in NaX with a loading degree of 0.08 at 350 K, a relatively sharp line at 9.7 ppm is observed and moreover a shoulder-like line appearing under the main CH_2 line at 3.8 ppm. It cannot be excluded that even for such small loading degrees there are some molecules which are not adsorbed inside the supercage but strongly hydrogen bonded to outer surface of the grains. A ^{1}H NMR line at 9.7 ppm can be caused by the displacement of the hydrogen bond of 0.35 Å from the exact middle of the OH···O hydrogen bond which corresponds to an O−O distance of 2.68 Å. The CH_2 group of such kind of species is also visible which is the line appearing as a shoulder under the broad line at 3.8 ppm. Because such species are strongly bonded to the outer surface, they are not able to exchange with the molecules inside the cages. At a higher pore-filling factor, $\Theta = 0.52$ (Figure 6 b), the spectra clearly show two intense lines typical for adsorbed EG molecules. But still the additional lines are visible as very weak peaks at 9.7, 2.5, and 1.3 ppm. As the number of molecules is increasing, the molecules adsorbed at the outside surface start to exchange and therefore it is difficult to detect them.

From now on, only the intense and relatively broad lines near 3.7 and 5.4 ppm (at 300 K) are considered, being attributed to the OH and CH_2 groups of EG molecules in the supercages. As Figure 5 reveals, the intensity ratio of $0.5{:}0.36 \cong 1.5$ which is less than the expected ratio of 2 for $\Theta = 0.2$. If we measure the same spectra at higher temperatures (Figure 6a), these lines are narrowed and the intensity ratio is closer to the ratio of 2:1 as expected for CH_2 and OH groups. Similar change in the relative intensities is also observed for a pore filling of $\Theta = 0.52$. We have found relative intensity ratios of the CH_2 to the OH group lines of 1.1:1 at 310 K, 1.6:1 at 330 K, 1.8:1 at 350 K, and 2:1 at 370 K. Because of the higher signal-to-noise ratio in the latter measurements, the numerical line deconvolution is less influenced by statistical errors, and since we have found a clear temperature dependence of these values, the change of the relative intensities is to be considered as an intrinsic effect (see below). Moreover, the line shift for the CH_2 group does not depend on the temperature while the OH group is shifting to higher fields with increasing temperature (4.9 ppm at 350 K, Figure 6b).

^{1}H Longitudinal Relaxation Studies. Using MAS NMR techniques, selective longitudinal relaxation time measurements were run for various types of adsorbed EG molecules. In Figure 8, the temperature dependence of proton longitudinal relaxation times is shown for EG molecules in NaX with $\Theta \approx 1.8$. Here, the measurements were selectively realized for OH and CH_2 groups of those EG molecules which are not confined in the supercages and are characterized by relatively sharp and well-separated proton NMR lines.

The calculation of the fitting curves (full lines in Figure 8) for the two Larmor frequencies is based on the Bloembergen−Purcell−Pound (BPP) theory, assuming a predominant proton−proton dipole interaction. Furthermore, we may suggest that the thermal motion can be described by using a spectral density function with a single correlation time τ_c, where the temperature dependence of which may be explained by an Arrhenius ansatz $\tau_c = \tau_{c0} e^{E_A/RT}$. According to this model, the proton relaxation rate $1/T_1$ given by the well-known formula

$$\frac{1}{T_1} = \frac{K}{\omega} \times \{j(\omega) + 4j(2\omega)\} \qquad (1)$$

where $K = 2/5\ \gamma^4 \hbar^2 I(I+1)\ 1/\langle r^6 \rangle$ and the reduced spectral density function $j(\omega)$ is given by $j(\omega) = \tau_c/[1 + (\omega\tau_c)^2]$. Here r stands for the distance between the two protons in the CH_2 group of EG molecules. The theoretical curve for the relaxation times measured at 100 MHz fits well to the experimental data when a preexponential factor of $\tau_{c0} = 2.5 \times 10^{-15}$ s is chosen. Moreover, the activation energy is estimated to be $E_A = 25$ kJ/mol, and this is a typical value for the energy that the OH group needs to make a hydrogen bonding. As seen in Figure 8, the validity of these assumptions can be checked satisfactorily by relaxation rate measurements at two different Larmor frequencies. A shift in the minimum is observed as also expected from the theory, i.e., $(T_1)_{min} = 0.082$ s at 235 K for 100 MHz and $(T_1)_{min} = 403$ ms at 270 K for 500 MHz. From the minimum values a correlation time of $\tau_c(400\ \text{K}) \approx 5 \times 10^{-11}$ s is estimated (see the discussion below). Furthermore, from the values of T_1 at the minima, e.g. $(T_1)_{min} \approx 0.082$ s at 100 MHz, a mean proton−proton distance of $\langle r^6 \rangle^{1/6} \approx 1.82$ Å may be estimated. This is in good agreement with the proton−proton distance within the CH_2 group (1.85 Å) of an isolated EG molecule. Hence, the proton relaxation is predominantly caused by the intramolecular proton−proton interaction. Apart from the limits of experimental accuracy, the remaining small difference in the distances might be caused by a small contribution due to intermolecular dipole interactions with protons in neighboring

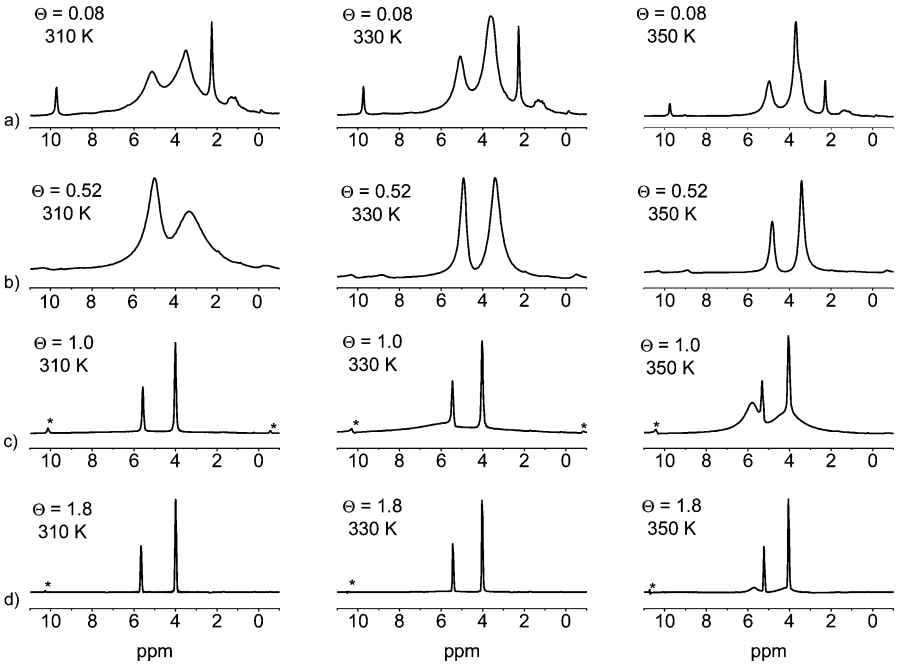

Figure 6. ^{1}H MAS NMR spectra (500 MHz, MAS frequency of 3 kHz) taken at 310, 330, and 350 K for different loading degrees: (a) $\Theta = 0.08$, (b) $\Theta = 0.52$, (c) $\Theta = 1.0$, and (d) $\Theta = 1.8$. * stands for the spinning sidebands.

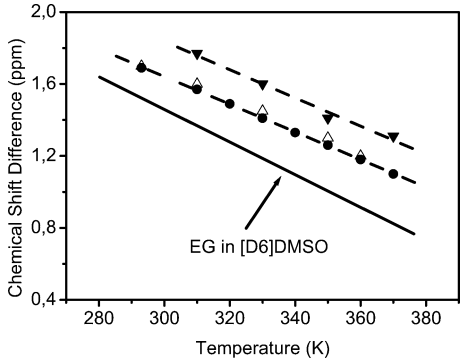

Figure 7. Chemical shift difference of OH and CH_2 groups of EG versus temperature plot for EG in DMSO-d_6 [ref 23] (solid line) and experimental data: Liquid EG ("EG in bulk") (filled circles), EG molecules which are at the outer surface of NaX for EG/NaX with $\Theta = 1.0$ (open triangles), and EG molecules which are adsorbed in the inner cages of NaX with $\Theta = 0.5$ (filled triangles).

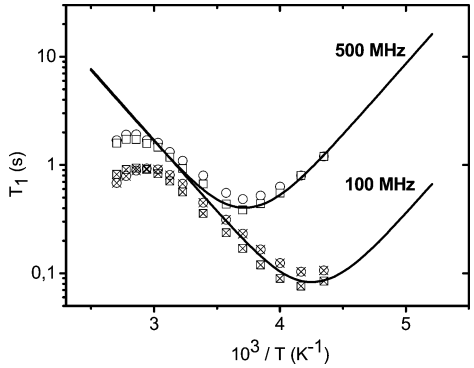

Figure 8. Temperature dependence of longitudinal proton relaxation time T_1 (100 and 500 MHz, MAS frequency of 3 kHz) for OH and CH_2 groups of EG molecules which are not adsorbed inside the supercages of NaX (loading $\Theta = 1.8$). Relaxation times for the OH group: at 100 MHz (open circles with cross) and at 500 MHz (open circles), for the CH_2 group: at 100 MHz (open squares with cross) and at 500 MHz (open squares). The full lines are fits according to eq 1.

molecular groups. The latter is apparently true when the relaxation times for the protons in the OH group are considered.

It is important to note that the proton longitudinal times T_1 for the OH and CH_2 groups behave similarly when the temperature is changed. They do not differ appreciably from each other and agree also nicely with the fits for two Larmor frequencies (Figure 8). The similar behavior of the relaxation times for the OH and CH_2 groups suggests that neither fast internal reorientational motions in the EG molecules nor a possible chemical exchange of the protons between OH groups in different EG molecules and with other hydrophilic sites in the zeolites plays any role for the proton relaxation. Hence, one may assume that the correlation time is connected with the movement of the molecule as a whole. Moreover, the isotropic character of the thermal motion might be understood if the respective molecules are relatively free to reorient or experience translational jumps with mean jump lengths much greater than the minimum proton distances in case of dominant intermoleculear proton−proton interactions.[27] Hence, the isotropic motion may also be considered to be a direct evidence for only a small restriction of the molecules, i.e., only a weak influence of confinement. This is reasonable, because we could already conclude from the proton chemical shift measurements that this behavior is typical for molecules which are adsorbed on the outer surfaces of the small zeolite grains.

A different situation arises for the proton relaxation times T_1 when EG molecules are adsorbed in NaX with a loading of $\Theta \approx 0.5$ (half filling) and $\Theta \approx 1.0$ (approximately complete filling of the supercages of the zeolite). In Figure 9 the respective relaxation times T_1 data for $\Theta \approx 0.5$ are displayed which are run at Larmor frequencies of 100 and 500 MHz. Because of the experimental limitations of our MAS probehead, we cannot extend the limits of the available temperature range. This is also the reason we cannot measure the relaxation times at 500 MHz at and above the temperature where the minimum occurs. But this lack of further data practically does not restrict our interpretation, because we could measure the relaxation times at 100 MHz where the minimum appears at ca. 400 K. From the frequency dependence of the relaxation times one may

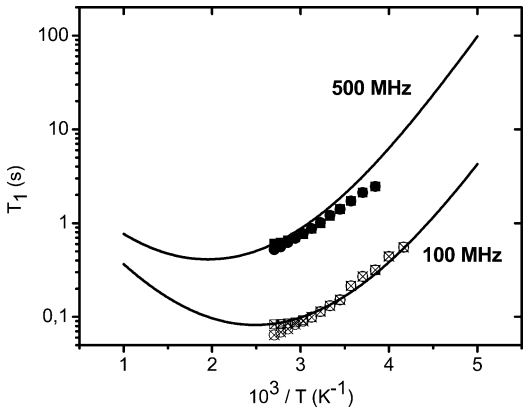

Figure 9. Temperature dependence of longitudinal proton relaxation time T_1 (100 and 500 MHz, MAS frequency of 3 kHz) for OH and CH_2 groups of EG molecules which are adsorbed inside the supercages of NaX (loading of $\Theta = 0.5$). Relaxation times for the OH group: at 100 MHz (open circles with cross) and at 500 MHz (filled circles), for the CH_2 group: at 100 MHz (open squares with cross) and at 500 MHz (filled squares). The full lines are fits according to eq 5.

immediately conclude that the data cannot be explained by applying a motional model with a single correlation time. We will show that the frequency and temperature dependence of the relaxation times can be explained by a distribution of correlation times τ_c. It is probable that this distribution is due to an energetic heterogeneity. Therefore, we apply the model of a log-normal distribution of τ_c which corresponds to a distribution of the activation energies E_c around its mean value $\langle E_c \rangle$,

$$\tau_c = \tau_{cm} \exp\left(\frac{E_c - \langle E_c \rangle}{RT}\right) \tag{2}$$

In a log-normal distribution of correlation times we have a Gaussian distribution of the quantity $z = \ln(\tau_c/\tau_{cm})$, viz.

$$\psi(z) = \frac{1}{\beta\sqrt{\pi}} \exp\left\{-\left(\frac{z}{\beta}\right)^2\right\} \tag{3}$$

where $\beta = \sqrt{2\langle z^2 \rangle}$ is the distribution parameter. It is well-known that for a distribution of correlation times, $j(\omega)$ in eq 1 is given by

$$j(\omega) = \int_0^\infty \psi(\tau_c) \frac{\omega\tau_c}{1 + (\omega\tau_c)^2} d\tau_c$$

This integral can be rewritten[28] as

$$f(x) = \omega j(x) = \frac{1}{\sqrt{\pi}} \int_{-\infty}^{+\infty} \frac{e^{-u2}}{e^{-(\beta u+x)} + e^{+(u+x)}} du \tag{4}$$

Here, the parameter x is defined by $x = \ln(\omega\tau_{cm})$. Thus, after some well-known straightforward calculations,[29] this expression leads to proton longitudinal relaxation rates T_1^{-1} in the form of

$$\frac{1}{T_1} = \frac{K}{\omega}\{f(x') + 2f(x' + 0.493)\} \tag{5}$$

where instead of the natural logarithm of x, the quantity

$$x' = \log_{10}(\omega\tau_{cm}) = \log_{10}(\omega\tau_{c0}) + 0.434\frac{\langle E_c \rangle}{RT}$$

is used. This is more convenient for the numerical analysis of the experimental data. Moreover, the integral limits of ± 4 instead of $\pm\infty$ may be used in eq 4, in the numerical calculations.

To maintain a quantitative agreement between the experimental data for EG in NaX with a loading degree of 0.5 and the relaxation model with a distribution of correlation times, at first, we have plotted the ratio $T_1/(T_1)_{min}$ as a function of x' for different values of β. In the measurements at 100 MHz, the minimum $(T_1)_{min}$ appears at approximately 400 K. Furthermore, it is known that for τ_{cm} it holds again $\omega\tau_{cm} = 0.62$ at $(T_1)_{min}$. This enables us to predict the correlation times τ_c for loading degree 0.5. From the theoretical fit, a preexponential factor of $\tau_{c0} \approx 6 \times 10^{-13}$ s for the correlation time is obtained. Thus, this gives a value of $(T_1)_{min} = 0.082$ s at a temperature of ca. 400 K measured at 100 MHz which is about the same as found for the more mobile molecules at $\Theta = 1.8$, i.e., we arrive again at a predominant intramolecular proton−proton interaction in the case of CH_2 groups. At the temperature of 400 K for $(T_1)_{min}$, τ_{cm} is estimated to be 9.9×10^{-10} s. Using these facts, proton relaxation times can be interpreted as follows: For both of the frequencies, 100 and 500 MHz, the best fit of the experimental T_1 curves as a function of temperature is obtained for $\beta = 3$, i.e., for a relatively high degree of heterogeneity. By definition, it holds $\tau_{cu}/\tau_{co} = e^{2\beta}$, where τ_{cu} and τ_{co} denote those correlation times for which the distribution function reduces to the $(1/e)$th part of its maximum value. For $\beta = 3$ this gives a ratio between the upper and lower values of $\tau_{cu}/\tau_{co} \approx 400$, i.e., a respective interval of correlation times from $\tau_{cu} \approx 8 \times 10^{-8}$ s to $\tau_{co} \approx 2 \times 10^{-10}$ s. Note that the correlation time $\tau_c(400\ K) \approx 5 \times 10^{-11}$ s for the mobile species in the system EG/NaX with $\Theta = 1.8$ is appreciably shorter than these both values. This situation is also clearly reflected in the quite different line widths for the molecules being adsorbed outside and inside the supercages. If we compare the minimum values $(T_1)_{min} \approx 0.082$ s estimated for pore-filling factors $\Theta = 1.8$ and $\Theta = 0.5$ at 100 MHz, we find practically no difference. Hence, we may estimate in both cases a mean proton−proton distance of $\langle r^6 \rangle^{1/6}$ for molecules adsorbed in the supercages which shows that the proton relaxation is dominated by intramolecular interactions modulated by rotational motion. This conclusion shows that a rotational motion of EG molecules is dominant in both cases. Apparently, the broad distribution cannot be related to the influence of a diffusion-like motion of the adsorbed molecules, where the minimum intermolecular proton−proton distance d is small with respect to the mean jump length $\langle l^2 \rangle^{1/2}$, i.e., $\langle l^2 \rangle/(12d^2) \ll 1$.[27] Since for EG/NaX samples with a loading degree of $\Theta = 0.5$ the majority of adsorbed molecules reveals a broad distribution of correlation times, we assume that the guest molecules are sterically hindered in the supercages of the NaX zeolites due to molecule−surface interactions. The latter influence is not observed for molecules assigned to be outside the cages (for $\Theta = 1.8$) which show clearly an isotropic motion in this temperature range. Hence, although the temperature range of our relaxation measurements at $\Theta = 0.5$ is limited we are able to derive unambiguous conclusions.

The differences between the dynamical behavior of EG molecules embedded in the supercages and the other types of adsorbed species can be directly seen if we measure the longitudinal relaxation times for samples where the ^{1}H NMR lines of both types of species can be simultaneously detected. This is shown in Figure 6c for $\Theta = 1.0$ measured above 310 K. If the MAS NMR measurements with this sample are run below 310 K, only the narrow line can be detected. When we measure the longitudinal relaxation times T_1 for the narrow lines

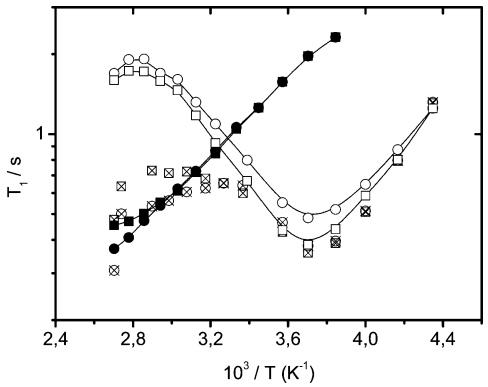

Figure 10. Temperature dependence of longitudinal proton relaxation time T_1 (500 MHz, MAS frequency of 3 kHz) for OH and CH_2 groups of EG molecules which are not adsorbed inside the supercages of NaX. Measurements at a loading of $\Theta = 1.8$: OH group (open circles), CH_2 group (open squares); at $\Theta = 1.0$: OH group (open circles with cross), CH_2 group (open squares with cross); for EG molecules which are adsorbed inside the supercages of NaX with $\Theta = 0.5$: OH group (filled circles), CH_2 group (filled squares). The solid lines are guides for the eyes.

(Figure 10), we find a temperature dependence at lower temperatures which is similar to that shown in Figure 8, i.e., we detect an isotropic motion as in the case of higher pore-filling factors (see e.g. the sample with $\Theta = 1.8$). On the other hand, at higher temperatures ($10^3/T < 3.4$) the behavior of the relaxation times for the narrow lines is changed. The relaxation times decrease now with increasing temperature similarly as found for the relaxation times of the broader lines observed in the samples with smaller pore-filling factors (see the filled symbols in Figure 10 and compare with Figure 9 for $\Theta = 0.5$). In order to understand this behavior, different effects have to be considered. We cannot assume that a fast or intermediate molecule exchange takes place, since we can always measure the narrow and broader lines separately. Hence, the exchange frequency should be smaller than the frequency differences given by the chemical shifts differences. Since the minimum shift difference for the CH_2 groups is 0.3 ppm or smaller, this would result in an exchange frequency of ca. 150 Hz (if we consider the NMR measurements at 500 MHz). Therefore, the mean residence time of the molecules in the temperature range of the T_1 measurements with respect to the molecule exchange should be ca. 10 ms or longer. With respect to the relaxation times (minimum values of ca. 0.082 s) it appears that we are already in the temperature range of intermediate or fast exchange. This explains why always purely exponential attenuation functions were obtained in the selective longitudinal relaxation measurements. Obviously, a fast cross-relaxation between the different species plays an important role. This situation may explain that the relaxation processes of the different molecular species are coupled so that always the process with the higher relaxation rate determines the effective longitudinal relaxation rate. For $\Theta = 1.0$, the latter is seen in the transition region near $10^3/T = 3.2$ in Figure 10. In this sense, the ^{1}H NMR T_1 relaxation measurements for $\Theta = 1.0$ include the results for all types of samples with loading degrees of $\Theta = 0.5$, $\Theta = 1.0$, and $\Theta = 1.8$ and, thus, the changes in the molecular mobility under the influence of confinement.

Discussion and Conclusion

The clear dependence of the ^{1}H MAS NMR spectra of EG adsorbed in NaX zeolites on the pore-filling degree gives the possibility to unambiguously characterize those molecules which are adsorbed in the supercages. Clear changes in the spectra for a pore filling close to $\Theta = 1.0$ appear which furthermore indicate that there is slow molecular exchange between these molecules and other types on the time scale of the chemical shift measurements. It is known that the number of adsorbed molecules, corresponding to e.g. $\Theta = 1.0$, may change with the temperature. In the temperature range of our measurements we are able to confirm the pore filling by inspecting ^{1}H NMR chemical shifts. Molecules sitting at the outer surface possess a much higher mobility which leads to relatively narrow and well-separated lines. EG molecules in the supercages are so strongly immobilized for higher loadings $\Theta > 1$ ("overloaded samples") that they can be detected in the MAS NMR spectra only at temperatures above 350 K (Figures 3 and 4). For samples with $\Theta < 1.0$, the line widths for the molecules in the supercages are smaller compared to those at higher loadings. Hence, the spectra are already detectable at lower temperatures (Figure 6 b). This may be explained because these molecules are not so closely "packed" in the supercages as in the case of complete pore filling, i.e., they have a greater mobility. Moreover, EG molecules within the supercages have typical chemical shifts which differ from those of the other adsorbed molecules.

For the case of EG in NaX with a filling factor of $\Theta = 0.52$ (Figure 6), the intensity ratio of 1.1 of CH_2 (at 3.7 ppm) and OH groups (at 5.2 ppm) strongly deviates from the expected value of 2 near room temperature. Only at 360 K could a ratio of 2:1 be measured. Now, the question is whether this result may be interpreted in a similar way to that of Hong et al.[21] who have studied the behavior of EG introduced into zeolites of sodalite type. In the ^{1}H NMR spectra they have found two peaks at 3.8 ppm (attributed to CH_2 groups) and 1.9 ppm (attributed to OH groups) with an intensity ratio of 2:1, i.e., quite different from the intensity ratios observed in Figure 1. They have suggested that a strong shift for the OH line occurs for EG in the beta-cages of sodalite, and this line appears at still higher fields than the CH_2 groups. This inversion of the line positions was also found[21] in case of strong (acidic) hydrogen bonds. Hong et al. explained this line positions in terms of strong conformational changes of EG in the beta-cages of sodalite. Since we did not find such a strong change in the ^{1}H NMR line shifts for the OH groups of EG in NaX with filling factors of $\Theta \approx 0.5$, we suggest another explanation for the intensity changes. We suppose that for samples with filling factors of $\Theta < 1.0$, a fraction of the CH_2 groups is not detectable because their proton NMR lines are strongly broadened. We explain this broadening by intramolecular dipole interactions because we may compare them with the lines for OH groups in the same species. The smaller line widths for the OH protons in this fraction of adsorbed molecules could be observed because these protons might be involved in exchange processes with neighboring OH groups in a time scale of milliseconds so that still a line narrowing occurs in contrast to the broader CH_2 group lines. Increasing the temperature, the molecular mobility of these species is drastically increased so that all molecules may contribute to the CH_2 group intensity observed. Thus, the peculiarities in the line intensities (Figures 6b and 6c) reflect also the complex equilibrium discussed already above.

We can finally confirm that it is possible to characterize EG molecules embedded in the supercages of the NaX zeolites besides those sitting on the outer surfaces of the zeolite grains because they possess a quite different molecular mobility. Molecules on the outer surfaces can be described by a thermal motion with one correlation time in contrast to the molecules within the restricted geometry which are characterized by a

broad distribution of correlation times. Since these conclusions were consistently derived from selective relaxation time measurements of the CH_2 and OH groups, there is no doubt that the motional processes are related to the dynamical behavior of the molecules as a whole. It might be well understood that molecules in the supercages with restricted mobility could reflect the dynamic heterogeneity in a much stronger way than the other types of adsorbed molecules which, moreover, can participate in exchange processes and thus might be the subject of effective averaging processes. Hence, we have shown that the dynamic heterogeneity may be related to the competing influences of interactions between molecules and internal surfaces and molecule-molecule interactions within a network of intermolecular hydrogen bonds.

Acknowledgment. The help of Dr. A. Pampel and Mr. G. Klotzsche in the performance of the NMR experiments is kindly acknowledged. The authors are indebted Dr. G. Buntkowsky (FU Berlin) for helpful discussions about the influence of hydrogen bonding in the chemical shifts, to Dr. W. Böhlmann for the synthesis of NaX zeolites, and to Mr. L. Moschkowitz for the guidance in the preparation of the samples used in the experiments.

References and Notes

(1) Engelhardt, G.; Michel, D. *High-Resolution Solid-States NMR of Silicates and Zeolites*; John Wiley & Sons: Chichester, 1987.

(2) Schwerk, U.; Michel, D.; Pruski, M. J. *Magn. Reson.* **1996**, *119*, 157−164.

(3) Roland, J.; Michel, D. *Magn. Reson. Chem.* **2000**, *38*, 587−595.

(4) Isfort, O.; Boddenberg, B.; Fujara, F.; Grosse, R. *Chem. Phys. Lett.* **1998**, *288*, 71−76.

(5) Kärger, J.; Heitjans, P.; Haberlandt, R. *Diffusion in Condensed Matter*; Friedr. Vieweg & Sohn Verlagsgesellschaft mbH: Wiesbaden, 1998.

(6) Dore, J.; Webber, B.; Strange, J.; Farman, H.; Descamps M.; Carpentier, L. *Physica A* **2004**, *333*, 10−16.

(7) Aksnes, D. W.; Kimtys, L. *Solid State NMR* **2004**, *25*, 146−152.

(8) Dosseh, G.; Xia, Y.; Alba-Simionesco, C. *J. Phys. Chem. B* **2003**, *107*, 6445−6453.

(9) Lusceac, S. A.; Koplin, C.; Medick, P.; Vogel, M.; Brodie-Linder, N.; LeQuellec, C.; Alba-Simionesco, C.; Rössler, E. A. C. *J. Phys. Chem. B* **2004**, *108*, 16601−16605.

(10) Kremer, F.; Huwe, A.; Arndt, M.; Behrens P.; Schwieger, W. *J. Phys. Cond. Mater.* **1999**, *11*, A175−A188.

(11) Rittig, F.; Huwe, A.; Fleischer, G.; Kärger J.; Kremer, F. *Phys. Chem. Chem. Phys.* **1999**, *1*, 519−523.

(12) Arndt, M.; Strannarius, R.; Groothues, H.; Hempel, E.; Kremer, F. *Phys. Rev. Lett.* **1997**, *79*, 2077−2080.

(13) Huwe, A.; Kremer, F.; Kärger, J.; Behrens, P.; Schwieger, W.; Ihlein, G.; Weiss O.; Schüth, F. *J. Mol. Liquids* **2000**, *86*, 173−182.

(14) Huwe, A.; Appelhans, D.; Prigann, J.; Voit, B. I.; Kremer, F. *Macromolecules* **2000**, *33*, 3762−3766.

(15) Baerlocher, C.; Meier, W. M.; Olson, D. H. *Atlas of Zeolites Framework Types*; Elsevier: Asmsterdam, 2001.

(16) Vogel, H. *Phys. Zeit.* **1921**, *22*, 645−646.

(17) Fulcher, G. S. *J. Am. Chem. Soc.* **1925**, *8*, 339−345.

(18) Huwe, A. Ph.D. thesis, University of Leipzig, 2000.

(19) Medick, P.; Blochowicz, T.; Vogel M.; Roessler, E. *J. Non-Cryst. Solids* **2002**, *310*, 565−572.

(20) Han, D. Y.; Woo A. J.; Nam, I. S.; Hong, S. B. *J. Phys. Chem.* B **2002**, *106*, 6206−6210.

(21) Hong, S. B.; Camblor M. A.; Davis, M. E. *J. Am. Chem. Soc.* **1997**, *119*, 761−770.

(22) Mildner, T.; Ernst H.; Freude, D. *Solid State NMR* **1995**, *5*, 269−271.

(23) Braun, S.; Kalinowski, H. O.; Berger, S. *150 and More Basic NMR Experiments*; Wiley-VCH: Weinheim, 1998.

(24) Brunner, E. *J. Mol. Struct.* **1995**, *355*, 61−85.

(25) Pimentel G. C.; McClellan, A. L. *The Hydrogen Bond*; W. H. Freeman and Company: New York, 1960.

(26) Emmler, T.; Gieschler, S.; Limbach, H. H.; Buntkowsky, G. *J. Mol. Struct.* **2004**, *700*, 29−38.

(27) Krüger, G. J. Z. *Naturf.* **1969**, *24a*, 560−565.

(28) Michel D.; Pfeifer, H. *J. Magn. Reson.* **1981**, *45*, 30−41.

(29) Pfeifer, H. *Nuclear Magnetic Resonance and Relaxation of Molecules Adsorbed on Solids*; Springer-Verlag Berlin: Germany, 1972; pp 68−90.